PB-759 350

ANGULAR RESOLUTION OF TWO TARGETS IN A PULSED SEARCH RADAR

James H. Hughen

Naval Research Laboratory

Prepared for:

Office of Naval Research

30 March 1973

NRL Report 7551

Angular Resolution of Two Targets in a Pulsed Search Radar

JAMES H. HUGHEN

Radar Analysis Staff
Radar Division

March 30, 1973

NAVAL RESEARCH LABORATORY
Washington, D.C.

Security Classification

DOCUMENT CONTROL DATA - R & D

(Security classification of title, body of abstract and indexing annotation must be entered when the overall report is classified)

1. ORIGINATING ACTIVITY *(Corporate author)* Naval Research Laboratory Washington, D.C. 20375	2a. REPORT SECURITY CLASSIFICATION Unclassified 2b. GROUP

3. REPORT TITLE

ANGULAR RESOLUTION OF TWO TARGETS IN A PULSED SEARCH RADAR

4. DESCRIPTIVE NOTES *(Type of report and inclusive dates)*
An interim report on a continuing NRL Problem.

5. AUTHOR(S) *(First name, middle initial, last name)*
James H. Hughen

6. REPORT DATE March 30, 1973	7a. TOTAL NO. OF PAGES 22	7b. NO. OF REFS 7
8a. CONTRACT OR GRANT NO. NRL Problem R02-54 b. PROJECT NO. RF-12-151-403-4010 c. d.	9a. ORIGINATOR'S REPORT NUMBER(S) NRL Report 7551 9b. OTHER REPORT NO(S) *(Any other numbers that may be assigned this report)*	

10. DISTRIBUTION STATEMENT
Approved for public release; distribution unlimited.

11. SUPPLEMENTARY NOTES	12. SPONSORING MILITARY ACTIVITY Office of Naval Research Department of the Navy Arlington, Virginia 22217

13. ABSTRACT

A generalized likelihood ratio test is used to find approximate limits on the angular resolution of two targets for a mechanically rotated antenna. The accuracy of maximum-likelihood azimuth estimates of the two interfering targets is also investigated. The results are found to be comparable to those obtained by directly processing the outputs of the individual elements of an antenna array.

A simple ad hoc procedure for angular resolution and estimation is also analyzed. The performance of the ad hoc test is found to be within 2 to 3 dB of that of the generalized likelihood ratio test.

DD FORM 1 NOV 65 1473 (PAGE 1)

S/N 0101-807-6801

Security Classification

Security Classification

14. KEY WORDS	LINK A		LINK B		LINK C	
	ROLE	WT	ROLE	WT	ROLE	WT
Angular resolution Search radar Generalized likelihood ratio test						

DD FORM 1 NOV 68 1473 (BACK)
(PAGE 2)

Security Classification

CONTENTS

ii

ABSTRACT

A generalized likelihood ratio test is used to find approximate limits on the angular resolution of two targets for a mechanically rotated antenna. The accuracy of maximum-likelihood azimuth estimates of the two interfering targets is also investigated. The results are found to be comparable to those obtained by directly processing the outputs of the individual elements of an antenna array.

A simple ad hoc procedure for angular resolution and estimation is also analyzed. The performance of the ad hoc test is found to be within 2 to 3 dB of that of the generalized likelihood ratio test.

AUTHORIZATION

NRL Problem R02-54
Project RF-12-151-403-4010

Manuscript submitted January 12, 1973.

ANGULAR RESOLUTION OF TWO TARGETS IN A PULSED SEARCH RADAR

INTRODUCTION

There has long been much interest in angular resolution of two point targets in radar and related fields. Investigators in many fields have sought ways to improve the angular resolution beyond the conventional 3-dB beamwidth limit (1 — 6), but none has been more successful than Ksienski and McGhee (5,6). Ksienski and McGhee reported that they were able to resolve two targets and obtain accurate angle estimates for target separations as small as a quarter beamwidth. They achieved this result by processing the quadrature components of the outputs of each element of a linear antenna array according to a generalized likelihood ratio test which tested for the presence of one or two targets.

It is of interest to determine whether performance comparable to that of Ksienski and McGhee's array processor can be obtained in a search radar using a mechanically rotated antenna. When the antenna rotates through a slowly fluctuating point target, the radar return consists of a sequence of pulses whose amplitude is modulated by the rotation pattern of the antenna and whose phase is random and independent from pulse to pulse. It is difficult to extract phase information from an incoherent pulse train, and the interest is in examining a radar which makes no attempt to do so. In other words, one assumes that the pulses are envelope detected prior to any resolution tests or target parameter estimations. On the other hand, in the array-processing work of Ksienski and McGhee, all phase information was used by obtaining estimates of the amplitude of the quadrature components of the target returns.

This report provides the results obtained using a generalized likelihood ratio test (GLRT) to test for the presence of one or two targets in the returns of a pulsed search radar with a mechanically rotating antenna. The envelope-detected pulses constitute the input data for the GLRT. The performance of this test is evaluated by computer simulation. In addition, an ad hoc test based on the duration of the radar returns above a detection threshold is evaluated and compared to the GLRT. The accuracy of the angle estimates of the two interfering targets is also calculated.

FORMULATION OF THE RESOLUTION TESTS

Mathematical Model

A two-dimensional (2-D) search radar which scans an azimuthal sector is considered. The sector may be a complete 360° circle or only a few degrees but is at least several times larger than the 3-dB beamwidth of the radar. A pulse is emitted at angular intervals of $\Delta\theta$. If enough pulses are emitted on a scan of the sector such that $\Delta\theta$ is small compared to the 3-dB beamwidth of the scanning antenna, then the returns from a stationary target

will be modulated by the antenna beam pattern. If one assumes that a single nonfluctuating* point target is present, then the return from the ith pulse can be written

$$r_i(t) = \gamma_1 f\left(\frac{\theta_i - \theta_{T1}}{\beta}\right) \cos\left[\omega_0 t + \phi(t) + \psi_{1i}\right] + n(t) \tag{1}$$

where

γ_1 is the maximum amplitude of the return signal (deterministic but unknown)

f is the modulation function, which depends on the antenna gain pattern

θ_i is the azimuth corresponding to the ith pulse

θ_{T1} is the actual target azimuth

β is a scale factor equal to half the null-to-null beamwidth

ω_0 is the frequency

$\phi(t)$ is the deterministic phase modulation (which may be present for pulse compression)

ψ_{1i} is the target phase angle, which is modeled as a uniformly distributed random variable independent from pulse to pulse

$n(t)$ is white Gaussian noise with spectral density $N_0/2$.

If instead of the single target of Eq. (1) there are two targets within the given range cell, then the return will be

$$r_i(t) = \sum_{\alpha=1}^{2} \gamma_\alpha f\left(\frac{\theta_i - \theta_{T\alpha}}{\beta}\right) \cos\left[\omega_0 t + \phi(t) + \psi_{\alpha i}\right] + n(t). \tag{2}$$

The target phase angle ψ_{2i} is also assumed to be a uniform random variable with pulse-to-pulse independence, and further, ψ_{2i} is assumed to be independent of ψ_{1i}.

The resolution problem as defined here is to detect the targets in such a manner as to identify whether Eq. (1) or Eq. (2) pertains. Also of interest is the related question concerning the accuracy of the azimuthal estimates when two targets are present.

The resolution problem is viewed as a problem in hypothesis testing. The hypothesis H_1, that one target is present, is to be tested against H_2, that two targets are present. This test is presumed to occur after a detection test has revealed the presence of at least one target.

Generalized Likelihood Ratio Test

The radar receiver in Fig. 1 is equivalent to a matched-filter/square-law envelope detector. The outputs of the envelope detector $\{y_i\}_{i=1}^{k}$ are assumed to comprise the available† data for the hypothesis test.

*Equivalently, the target can be modeled as a scan-to-scan fluctuating target having a prior amplitude distribution which is unknown or which contains unknown parameters.

†The number of pulses available, k, will depend on the pulse repetition frequency and on the scan rate.

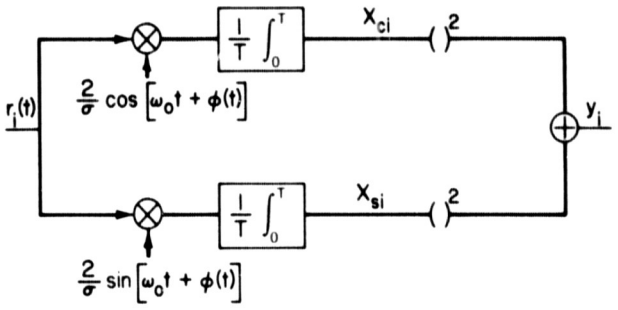

Fig. 1 — Correlation receiver equivalent of a matched filter/envelope detector

A likelihood ratio test is a statistical hypothesis test in which the test statistic is formed from the ratio of the joint probability density functions of the observations under both hypotheses, i.e.,

$$\Lambda = \frac{p[y_1, y_2, \ldots y_k \mid H_2]}{p[y_1, y_2, \ldots y_k \mid H_1]}, \tag{3}$$

where $p[y_1, y_2, \ldots y_k \mid H_j]$ is the joint probability density function or likelihood of the observations under hypothesis H_j. The decision is made by computing the value of test statistic Λ and comparing the result to some threshold. If the threshold is exceeded, the decision is "two targets present," and if the threshold is not exceeded the decision is "one target present."

In the appendix it is shown that the density of a single observation is noncentral chi-square with two degrees of freedom and a noncentrality parameter which is hypothesis dependent. Under H_1 the noncentrality parameter λ_{1i} is

$$H_1: \ \lambda_{1i} = \frac{\gamma_1^2}{\sigma^2} f^2\left(\frac{\theta_i - \theta_{T1}}{\beta}\right), \tag{4}$$

where σ^2 is the mean square noise level. Under H_2 the noncentrality parameter is approximately

$$H_2: \ \lambda_{2i} = \sum_{\alpha=1}^{2} \frac{\gamma_\alpha^2}{\sigma^2} f^2\left(\frac{\theta_i - \theta_{T\alpha}}{\beta}\right). \tag{5}$$

As shown in the appendix, the exact noncentrality parameter under H_2 contains a term proportional to the phase difference of the two targets, but the target phase angles are unknown and cannot be estimated under the assumptions made here. The correct method (from the Bayesian point of view) for eliminating this term is to find the ensemble average of $p[y_i/H_2]$ with respect to the target phase angles, as discussed in the appendix. The resulting integration is not a standard integral, and hence it was decided to simply take the ensemble average of the noncentrality parameter instead of the entire density function.

Since the likelihood ratio processor is specified by a ratio of probability density functions, the effect of approximating a density function is to make the resulting processor only an approximate likelihood ratio processor. The performance of the resulting processor seems to justify the approximation.

Since the pulses are assumed to be independent, the joint probability density is just the product of the densities of the individual observations. That is

$$p[y_1, y_2, \ldots y_k \mid H_j] = \prod_{i=1}^{k} p[y_i \mid H_j]$$

$$= \frac{1}{2^k} \exp\left[-\frac{1}{2}\sum_{i=1}^{k} (y_i + \lambda_{ji})\right] \prod_{i=1}^{k} I_0\left(\sqrt{\lambda_{ji}\, y_i}\right), \tag{6}$$

where I_0 is the modified Bessel function of the first kind with zero order.

Now to compute the value of the test statistic for a particular set of measurements, the likelihoods are computed by substituting the measurement values into the right-hand side of Eq. (6). The noncentrality parameter must also be evaluated and substituted into Eq. (6). One notices that to compute the values of the noncentrality parameter, knowledge of the target-return amplitudes γ_1 and γ_2 and of the target azimuth angles θ_{T1} and θ_{T2} is required. These target parameters are unknown, but their values can be estimated from the radar returns; the estimates can be used in lieu of actual parameter values to evaluate the noncentrality parameters. The use of maximum likelihood estimates of these parameters is the distinguishing feature of the generalized likelihood ratio test. Maximum likelihood estimates are obtained by finding the values of the parameters which yield a global maximum of the likelihood functions.

To analyze the performance of the GLRT, it is necessary to compute the probability density of the test statistic Λ under both H_1 and H_2. The probabilities of correct resolution P_R and of false resolution P_{FR} can then be computed as a function of target amplitudes and angular separation. The probability of correct resolution is given by

$$Pr\ [\text{CORRECT RESOLUTION}] \triangleq P_R = Pr\ [\Lambda > C \mid H_2], \tag{7}$$

and false resolution is

$$Pr\ [\text{FALSE RESOLUTION}] \triangleq P_{FR} = Pr\ [\Lambda > C \mid H_1]. \tag{8}$$

The difficulties encountered in finding the densities of the test statistic were formidable, and an alternative approach was adopted, namely, analysis by computer simulation.

Since azimuth estimates are found as a step in the resolution test, azimuth accuracy is readily investigated simply by examining the error variance of the maximum likelihood estimates.

Time-Above-Threshold Test

Though the GLRT described previously will provide an approximate bound on the resolution performance, it is likely that the capability to process real-time signals in this manner would be very costly. But whether or not, it is useful to compare the resolution performance of a simpler processing operation to that of the GLRT. One such resolution test is designated as the time-above-threshold test or TAT test. This test is based on a procedure which the radar operator might intuitively use. Following the envelope detector, a sliding-window type of integrator sums n pulses from a given range cell; the integrator output is then ordinarily compared to a detection threshold. As the search radar scans by a target, the integrator output will show a time dependence similar to that in Fig. 2. For very strong signals, the presence of two targets would be apparent to an operator viewing this type of display, provided that the two targets were sufficiently separated in azimuth. One might suspect that if the information in this type of display is examined more carefully, two targets can be resolved even when the returns are rather weak and the targets are separated by less than a beamwidth.

It turns out that by simply examining the time above threshold and the peak output, one is able to resolve two targets and to estimate remarkably well the azimuth angles of the two resolvable targets. The mean time above threshold as a function of integrator peak output for several values of target separation is required as a priori information. This information serves as a set of calibration curves. When an estimate is to be made for a particular scan, the obtained time above threshold and the integrator peak output are then used to find from the calibration curves the target separation which produces, on the average, this time above threshold.

SIMULATION RESULTS

Simulation Details

The performance analyses of both the GLRT and TAT resolution tests were conducted by computer simulation. To determine the probability of resolution, the data was generated for the condition two targets present, H_2. For each pulse, two independent, zero-mean, unit-variance, normal random variables were generated corresponding to the quadrature

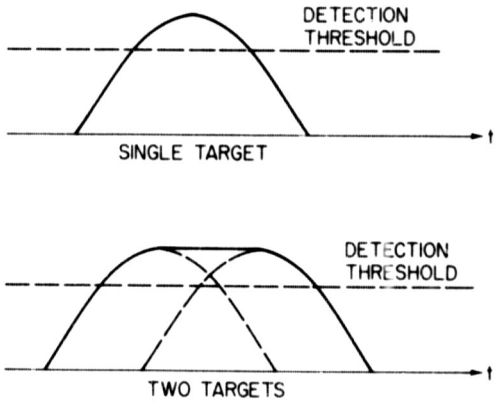

Fig. 2 — Integrator output showing response for one and two targets

components x_{ci} and x_{si} of Fig. 1. The mean values μ_{ci} and μ_{si} were then computed according to

$$\mu_{ci} = \sum_{\alpha=1}^{2} \frac{\gamma_\alpha}{\sigma} f\left(\frac{\theta_i - \theta_{T\alpha}}{\beta}\right) \cos \psi_{\alpha i} \tag{9a}$$

$$\mu_{si} = \sum_{\alpha=1}^{2} \frac{\gamma_\alpha}{\sigma} f\left(\frac{\theta_i - \theta_{T\alpha}}{\beta}\right) \sin \psi_{\alpha i} \tag{9b}$$

and added to the zero-mean random variables. Equations (9a) and (9b) are derived in the appendix. To compute the means μ_{ci} and μ_{si}, a specific scan pattern $f(.)$ must be chosen. The pattern used in these simulations was

$$f(x) = \frac{\sin \pi x}{\pi x}, \quad -1 \leqslant x \leqslant 1 \tag{10a}$$

and

$$f(x) = 0, \text{ otherwise.} \tag{10b}$$

This scan pattern is seen to be that portion of the curve lying between the first nulls. Using this definition of f, the scale factor β is specified such that the null-to-null beamwidth equals 2β, i.e., $f(\theta/\beta)$ is a null when $\theta = \pm \beta$.

The phase angles ψ_{1i} and ψ_{2i} are generated using a uniform random-number generator. The simulated quadrature components are then squared and added to form the envelope-detector outputs.

The number of pulses in each data set was variable, depending on target separation, but chosen so that 30 pulses would occur between the antenna-pattern nulls for a single target.

The test statistic is computed and then compared to a threshold value of 2.0, which gives a P_{FR} of less than approximately 0.04 for $\gamma/\sigma \leqslant 10$.* The false-resolution probability is dependent on the signal-to-noise ratio for a constant threshold.

The TAT test is performed after first integrating 10 pulses. If the envelope-detector output is y_i, then the integrator input z_i is

$$z_i = \sum_{j=1}^{10} y_{i+1-j}, \tag{11}$$

*The threshold value and the corresponding false resolution probability were determined by computer simulation.

which is compared to a detection threshold. The detection threshold corresponds to a false-alarm probability of $P_F = 10^{-6}$ in these simulations. If at least one detection threshold crossing occurs, then the duration of the excursion above threshold is calculated. This calculation is made by designating the first pulse of the (integrated) data set to cross the threshold as N_f and the last pulse exceeding the threshold as N_ℓ. The length N_d of the excursion above the threshold is then given by

$$N_d = N_\ell - N_f + 1. \tag{12}$$

The resolution test is then made by comparing N_d to a resolution threshold.

The resolution threshold for the TAT test is determined as follows. First the average length of the excursion above the detection threshold for the single-target case is estimated by running 50 trials at each of several signal-to-noise ratios. Then N_d is determined on each trial, and the results are averaged. This result is shown in Fig. 3 as the curve labeled "Single Target." The variance of N_d for the single-target case is also estimated, and the curve corresponding to the mean plus two standard deviations is constructed. This curve becomes the resolution threshold. The reason for making this curve the resolution threshold is simply that for a single target, the probability that N_d falls below the resolution threshold is about 97.7%. To express it another way, the probability that the resolution threshold will be exceeded in the single-target case is about 0.023, i.e., $P_{FR} \approx 0.02$. The resolution threshold vs integrator peak output is stored in the simulation program.

Estimation of target azimuth angles is accomplished as a part of the resolution test for the GLRT; however, the TAT test requires more processing in addition to that required for resolution. Azimuth estimation in the TAT test requires three more curves as a function of integrator peak output, specificaliy the average sequence length above (detection) threshold for one, one-half, and one-quarter beamwidth target separations. The curves are

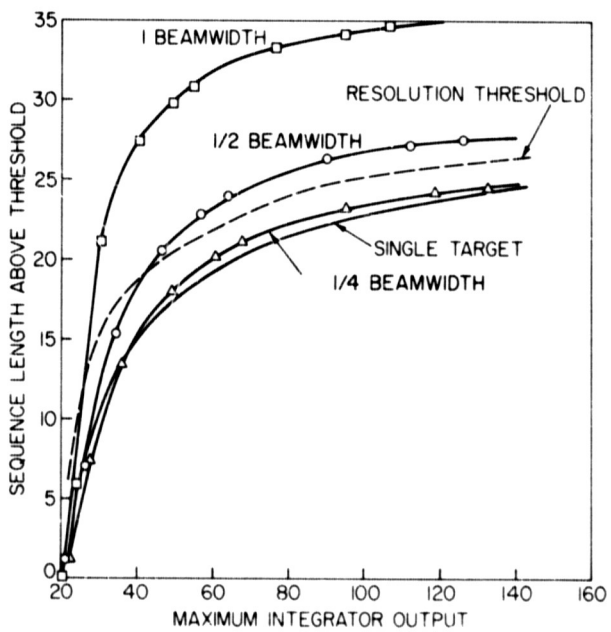

Fig. 3 — Sequence length above detection threshold vs integrator peak output

all shown in Fig. 3.* When a particular data set is processed, the sequence length above threshold N_d and the integrator peak output are found and in effect looked up in the graph of Fig. 3. If N_d falls above the resolution threshold, then the presence of two targets is assumed, and the separation in beamwidth is found via interpolation.

The curves of sequence length above threshold vs integrator peak output were obtained for equal-strength targets; however, good estimation results were obtained when the actual targets strengths were unequal.

Resolution Results

Figures 4a — 4c show the estimated probability $\hat{P}$ of resolving two targets using the GLRT. Each point on these curves represents the average of 50 independent trials. The 95%-confidence interval for P is ± 0.14 at $P = 0.5$ and decreases to ± 0.09 for $P = 0.1$ or $P = 0.9$. The four curves on each graph are labeled $\gamma_2/\gamma_1 = 1$, 0.5, 0.2, and 0.1; $N = 13$ indicates that there were 13 pulses within the 3-dB beamwidth. This corresponds to 30 pulses within the null-to-null beamwidth. Figures 5a and 5b show the corresponding resolution probabilities for the TAT test. As one might expect, at the lower signal-to-noise ratios, the GLRT shows better resolution performance in every case. However, for some cases at the higher signal-to-noise ratios, the TAT test performs as well as the GLRT. Specifically, comparing the two tests in Figs. 4a and 5a, it is seen that for $\gamma_2/\gamma_1 = 1$ and $\gamma_2/\gamma_1 = 0.5$ the TAT test actually shows some slight improvement over the GLRT at the higher values of signal-to-noise ratio. In this regard three observations are made: (a) The 95%-confidence interval for $P = 0.9$ is ± 0.09, so that some of the disparity may be statistical and hence more apparent than real. (b) It is well known that the GLRT is not a Uniformly Most Powerful (UMP) test (7). Indeed, for some parameter values the TAT test may be the more powerful. (c) Some approximations were made in the equations for the test statistic of the GLRT which could account for some performance degradation.

For the half-beamwidth-separation case of Figs. 4b and 5b, the GLRT appears to be uniformly more powerful than the TAT test. The TAT test failed to give useful results for the case of quarter-beamwidth separation.

Figure 2 of Ref. 5 has been replotted as Fig. 6 so that the abscissa reflects the signal amplitude-to-noise ratio which would have been measured had a beamformer been used. This change of abscissa permitted a more direct comparison with the present work. Figure 6 is the result obtained by Ksienski and McGhee for an 11-element array with a target spacing of one-half beamwidth. The corresponding result of the present work, Fig. 4b, shows a few dB improvement over the Ksienski result, which indeed is to be expected, since in the mechanical-scan case, 13 pulses occur within the 3-dB beamwidth, whereas Ksienski's result is for a single pulse.

Figure 7 shows the signal amplitude-to-noise ratio required to achieve a 0.5 probability of resolution for $\gamma_1 = \gamma_2$. If one takes into account the postdetection integration gain of 5 to 6 dB for the GLRT, then the results of Ksienski and McGhee will show a 1- to 3-dB performance advantage over the GLRT. It should be noted for the results of Ref. 5 that the probability of false resolution P_{FR} is not known exactly, although the authors state that it is acceptably low.

*Unless stated otherwise, beamwidth refers to the 3-dB points on the antenna pattern.

(a) One beamwidth

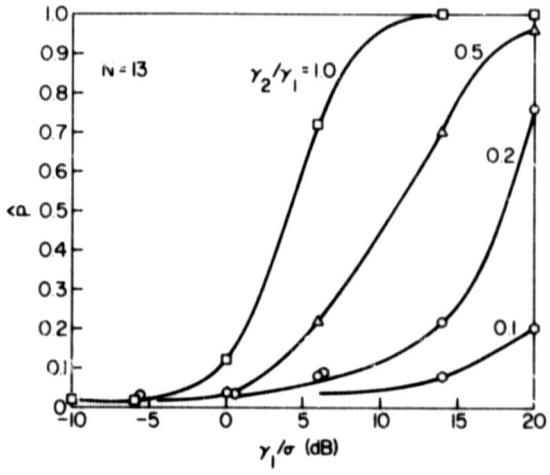

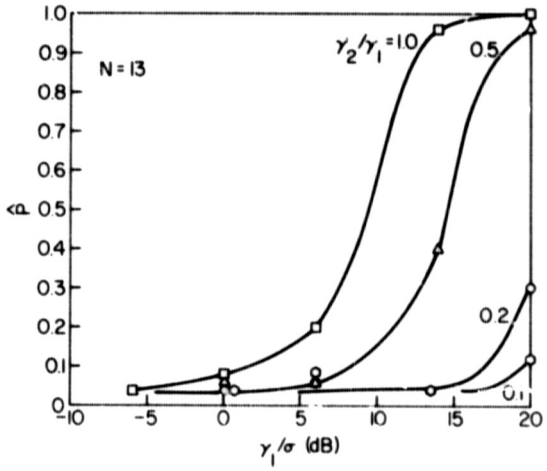

(b) Half beamwidth

(c) Quarter beamwidth

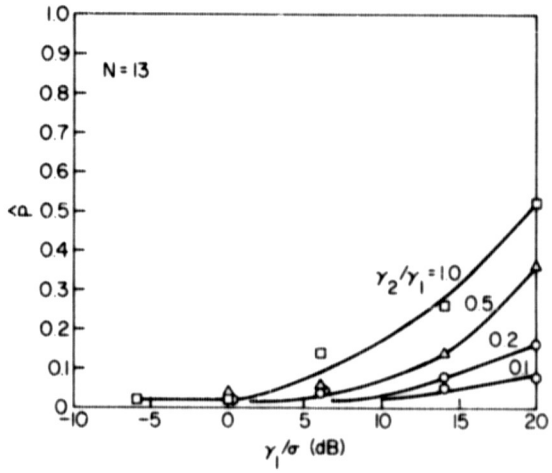

Fig. 4 — Probability of resolving two targets using GLRT for three target separations

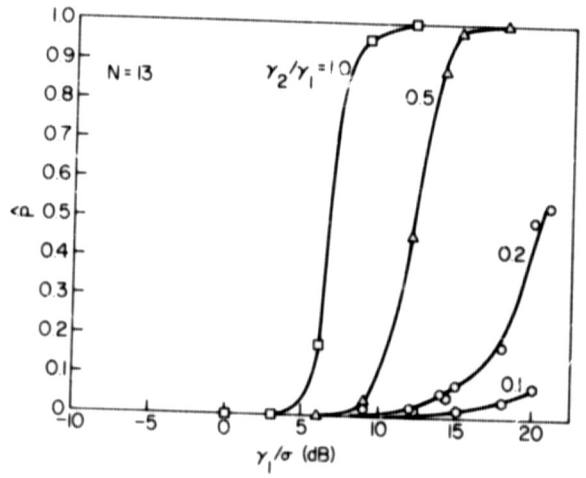

(a) One beamwidth

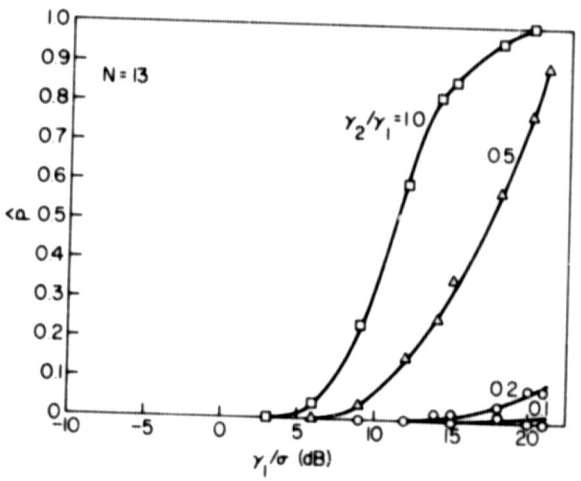

(b) Half beamwidth

Fig. 5 — Probability of resolving two targets using TAT test for two target separations

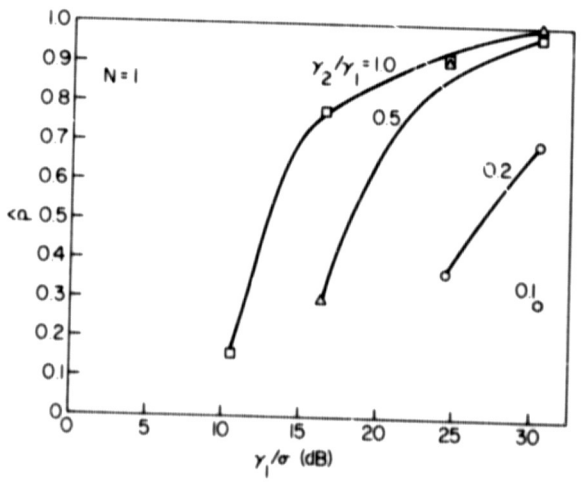

Fig. 6 — Probability of resolving two targets separated by half beamwidth for an 11-element array (from Ksienski and McGhee (5))

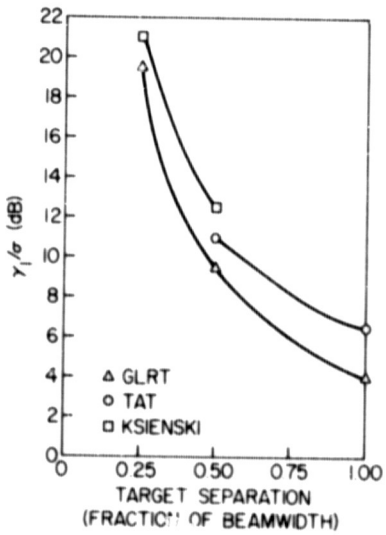

Fig. 7 — Signal amplitude-to-noise ratio required for 0.5 probability of resolution vs target separation

The target phase angles ψ_{1i} and ψ_{2i} are assumed to be independent in the derivation of the test statistics for both the GLRT and the TAT test. It is interesting to compare the performance of the tests when the target phase angles have a fixed relationship, i.e., when $\psi_{2i} = \psi_{1i} + \eta$, where η is a constant. Figures 8a and 8b show the resolution performance for several values of η for a half-beamwidth target separation. The TAT test is affected more than the GLRT by the nonrandom phase difference. Indeed, according to Figs. 8a and 8b, there is little degradation of the GLRT, whereas the TAT test is degraded significantly for small η. It is quite likely that the TAT test performance can be improved for this case where $\psi_{2i} = \psi_{1i} + \eta$ if this relationship is considered in the generation of the calibration curves of Fig. 3.

Angular-Estimation Results

Figures 9 through 12 show the rms error in the azimuth-angle estimates for the GLRT and TAT tests. All of these graphs are normalized with respect to the 3-dB beamwidth. The rms error is defined as the square root of the mean-square error (MSE). For target-1 azimuth,

$$MSE = \frac{1}{M} \sum_{j=1}^{M} \left(\frac{\hat{\theta}^j_{T1} - \theta_{T1}}{B} \right)^2, \tag{13}$$

where M is the total number of resolutions which occurred in the 50 Monte Carlo trials, θ_{T1} is the true azimuth of target 1, $\hat{\theta}^j_{T1}$ is the estimate of azimuth 1 obtained on the jth resolution, and B is the 3-dB beamwidth of the antenna scan pattern. As Eq. (13) indicates, unless both targets are detected, i.e., resolved, the azimuth estimates are not included in the results shown. Only points which correspond to at least 10 resolutions are plotted.

Figures 9a and 10a are for a one-beamwidth separation of the two targets. The maximum-likelihood (ML) estimates are somewhat more accurate than the TAT estimates for this case, as might be expected. However, for the case of half-beamwidth separation, the reverse is true.

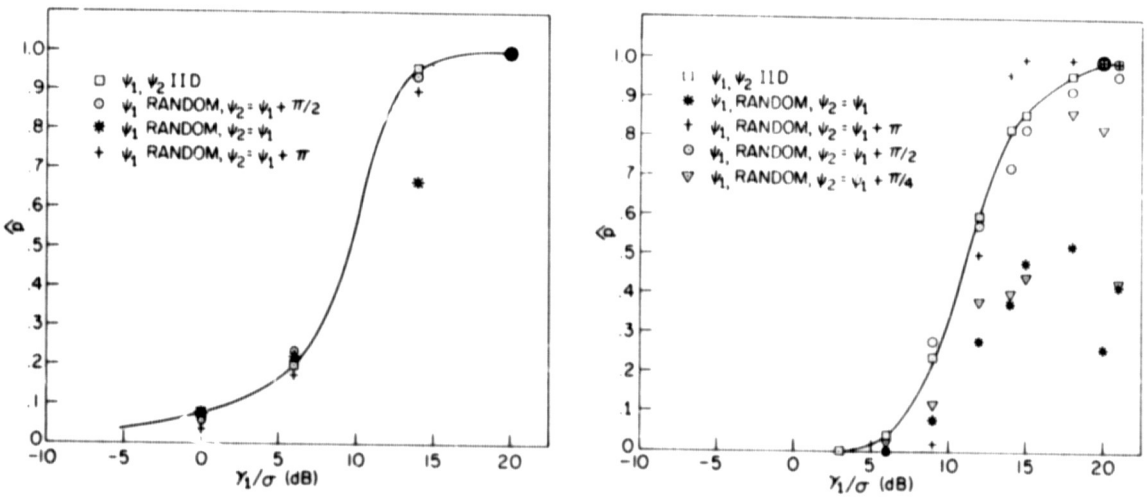

(a) GLRT (b) TAT test

Fig. 8 — Probability of resolving two targets separated by half beamwidth for several target phase angle relationships using two tests

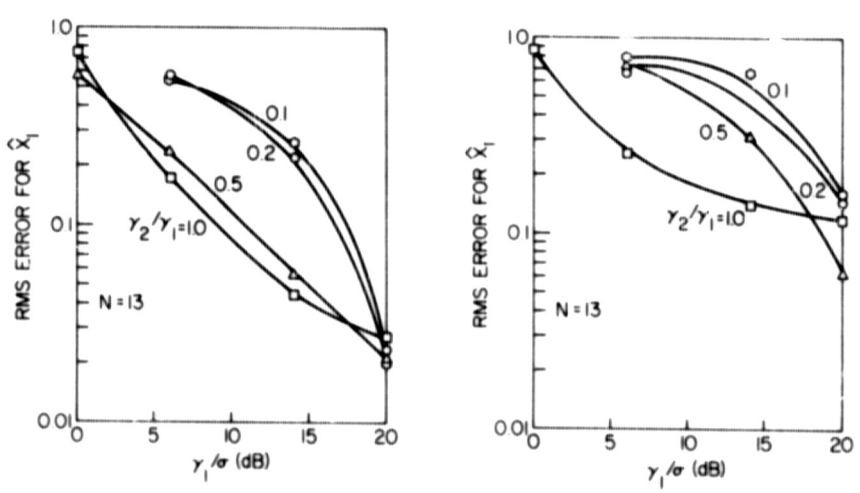

(a) One beamwidth (b) Half beamwidth

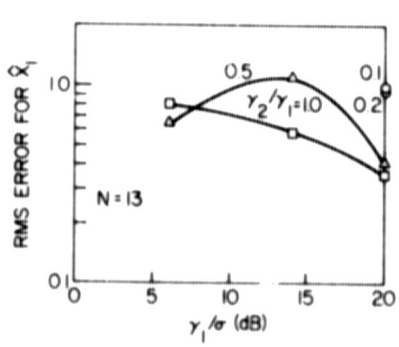

(c) Quarter beamwidth

Fig. 9 — Root-mean-square error in ML estimates of target-1 azimuth for three target separations

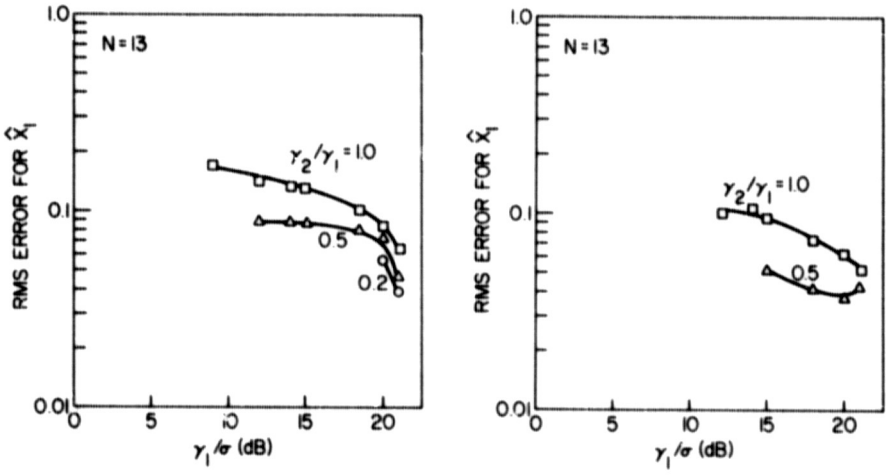

(a) One beamwidth (b) Half beamwidth

Fig. 10 — Root-mean-square error in TAT estimate of target-1 azimuth for two target separations

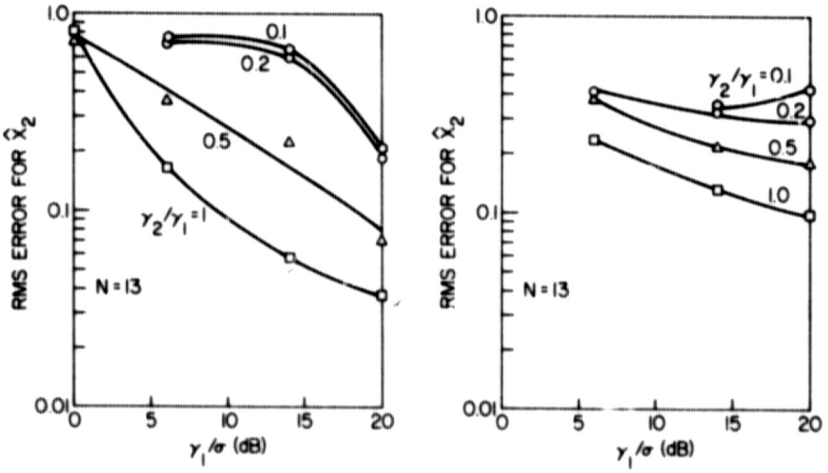

(a) One beamwidth (b) Half beamwidth

Fig. 11 — Root-mean-square error in ML estimate of target-2 azimuth for two target separations

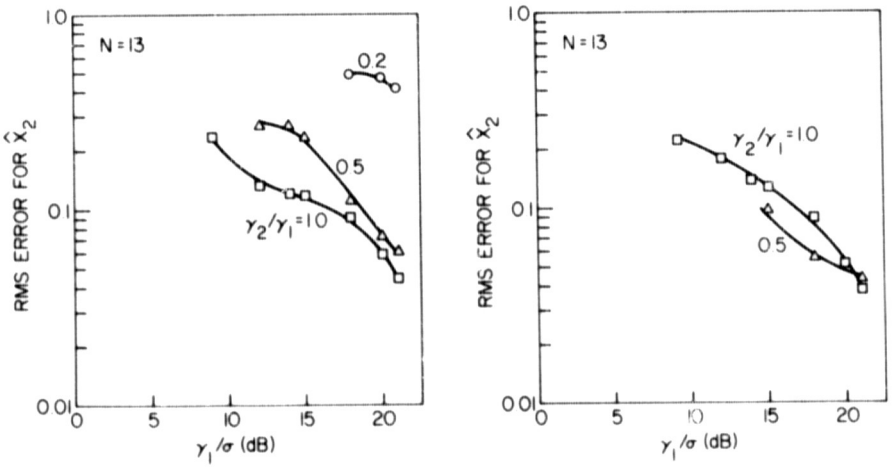

(a) One beamwidth (b) Half beamwidth

Fig. 12 — Root-mean-square error in TAT estimate of target-2 azimuth for two target separations

The TAT estimates of target-1 azimuth in Fig. 10 show an increase in accuracy as the target ratio γ_2/γ_1 decreases. However, the corresponding ML estimates of Fig. 9 do not show the same trend. Another notable point is that the TAT estimates appear to be approximately equally accurate in the one-beamwidth separation and the half-beamwidth separation cases, whereas the ML estimates show a definite degradation as target separation decreases.

The estimation error for target 2 is shown in Figs. 10 and 11. One notes that the rms error increases as the ratio γ_2/γ_1 decreases. This is the proper trend, since decreasing γ_2 is equivalent to decreasing the signal-to-noise ratio of the return from target 2.

CONCLUSIONS

One of the objectives of this investigation was to compare the angular-resolution results for a mechanically scanned antenna to those results obtained for the direct processing of the array-element outputs. It was found that, indeed, the angular resolution capability of the mechanical scan is comparable to that obtained by direct array processing. Further, the results presented here indicate that reliable resolution can be obtained for targets spaced as close as a half beamwidth. This is in contrast to the conclusion of Ksienski and McGhee (6) who suggested that reliable resolution could be obtained with modest signal-to-noise ratio for target spacings down to a quarter beamwidth.

Comparison with their results should be made by considering the signal-to-noise ratios which would result from summing the outputs of the elements of their array rather than individual element signal-to-noise ratios. On this basis their results, as well as those presented here, indicate that a very large signal-to-noise ratio is required for resolution at a quarter beamwidth.

Though the GLRT used in this study is considered impractical in its present form, there are means to shorten the computation time and to reduce the complexity of implementation. For example, instead of the gradient method used to maximize the likelihoods,

a finite grid search could be devised. This approach worked well for Ksienski and McGhee. On the other hand, the resolution performance of the more readily implementable TAT procedure was within 2 to 3 dB of the GLRT for a resolution probability of 0.5, and hence future efforts would probably be more fruitful concentrating on the TAT test rather than on the GLRT.

The analysis presented here dealt with an idealized target model in a background of white noise. Extension of the analysis to targets spread in range or doppler in a clutter background would be a very difficult task. A more feasible problem would be to analyze the performance degradation of the present GLRT and TAT test in a realistic environment.

ACKNOWLEDGMENT

This study owes its existence to Dr. G. V. Trunk. It was he who posed the problem, and the TAT test is his conception. I gratefully acknowledge his encouragement and helpful discussion throughout the course of this investigation. Also, I thank my colleagues H. A. Brown, D. D. Howard, and J. P. Barry for their review and constructive comments on this report.

REFERENCES

1. C.J. Bouwkamp and N.G. de Bruijn, "The Problem of Optimum Antenna Current Distribution," Philips Research Reports 1, 135 (1946).
2. J. Freedman, "Resolution in Radar Systems," Proc. IRE, 39, 813 (1951).
3. A. Berman and C.S. Clay, "Theory of Time-Averaged Product Arrays," J. Acoust. Soc. Amer. 29, 806 (1957).
4. P. Swerling, "The Resolvability of Point Sources," Rand Corporation Report, 1862 Dec. 1959.
5. A.A. Ksienski and R.B. McGhee, "Radar Signal Processing for Angular Resolution Beyond the Rayleigh Limit," The Radio and Electronic Engineer 34, 161 (1967).
6. A.A. Ksienski and R.B. McGhee, "A Decision Theoretic Approach to the Angular Resolution and Parameter Estimation Problem for Multiple Targets," IEEE Trans. AES 4, No. 3, 443 (1968).
7. H.L. Van Trees, "Detection, Estimation, and Modulation Theory," Part I, John Wiley and Sons, New York, 1968.

Appendix

DISTRIBUTION OF ENVELOPE DETECTOR OUTPUT

In this appendix the probability distribution of the output y_i of the square-law envelope detector will be derived. The input to the radar receiver under H_1 is given by Eq. (1), which is rewritten here for convenience:

$$H_1: \; r_i(t) = \gamma_1 f\left(\frac{\theta_i - \theta_{T1}}{\beta}\right) \cos\left[\omega_0 t + \phi(t) + \psi_{1i}\right] + n(t). \tag{A1}$$

Referring to Fig. 1, the quadrature components x_{ci} and x_{si} are seen to be

$$x_{ci} = \frac{\gamma_1}{\sigma} f\left(\frac{\theta_i - \theta_{T1}}{\beta}\right) \cos \psi_{1i} + \frac{1}{T}\int_0^T n(t)\,\frac{2}{\sigma} \cos\left[\omega_0 t + \phi(t)\right]\, dt \tag{A2a}$$

and

$$x_{si} = \frac{\gamma_1}{\sigma} f\left(\frac{\theta_i - \theta_{T1}}{\beta}\right) \sin \psi_{1i} + \frac{1}{T}\int_0^T n(t)\,\frac{2}{\sigma} \sin\left[\omega_c t + \phi(t)\right]\, dt. \tag{A2b}$$

Since $n(t)$ is Gaussian white noise with $E[n(t)n(u)] = (N_0/2)\,\delta\,(t-u)$, both x_{ci} and x_{si} in Eqs. (A2a) and (A2b) are conditionally normally distributed (given ψ_{1i}) with means μ_{ci} and μ_{si} respectively, where

$$\mu_{ci} = \frac{\gamma_1}{\sigma} f\left(\frac{\theta_i - \theta_{T1}}{\beta}\right) \cos \psi_{1i} \tag{A3a}$$

and

$$\mu_{si} = \frac{\gamma_1}{\sigma} f\left(\frac{\theta_i - \theta_{T1}}{\beta}\right) \sin \psi_{1i}. \tag{A3b}$$

The variance of x_{ci} is

$$\text{var}\,(x_{ci} \mid \psi_{1i}, H_1)$$

$$= E\left\{\frac{4}{\sigma^2 T^2}\int_0^T \int_0^T n(t)n(u) \cos\left[\omega_0 t + \phi(t)\right] \cos\left[\omega_0 u + \phi(u)\right]\, dt \right. \tag{A4a}$$

$$= \frac{4}{\sigma^2 T^2}\int_0^T \frac{N_0}{2} \cos^2\left[\omega_0 t + \phi(t)\right]\, dt \tag{A4b}$$

$$= \frac{N_0}{\sigma^2 T}. \tag{A4c}$$

By definition the noise power σ^2 is the product of the noise spectral density $N_0/2$ and the noise equivalent bandwidth, which is approximately $1/T$. Therefore

$$\sigma^2 = \frac{N_0}{T}, \tag{A5}$$

and hence

$$\text{var } (x_{ci} \mid \psi_{1i} H_1) = \text{var } (x_{si} \mid \psi_{1i} H_1) = 1. \tag{A6}$$

The output of the envelope detector is the sum of the squares of two nonzero-mean, unit-variance, normally distributed random variables and thus is distributed according to the noncentral chi-square distribution with two degrees of freedom and noncentrality parameter λ_{1i}, that is, under H_1:

$$H_1: \; y_i \sim \chi_2^2, \lambda_{1i},$$

where

$$\lambda_{1i} = \mu_{ci}^2 + \mu_{si}^2 = \frac{\gamma_1^2}{\sigma^2} f^2 \left(\frac{\theta_i - \theta_{T1}}{\beta}\right). \tag{A7}$$

One notes that this result is independent of target phase ψ_1. Price* gives a closed-form expression for the noncentral chi-square density:

$$p(y_i \mid H_1) = \frac{1}{2} \exp \left[\frac{-(y_i + \lambda_{1i})}{2}\right] I_0 \left(\sqrt{\lambda_{1i} y_i}\right). \tag{A8}$$

Under H_2, the radar return is

$$r_i(t) = \gamma_1 f \left(\frac{\theta_i - \theta_{T1}}{\beta}\right) \cos \left[\omega_0 t + \phi(t) + \psi_{1i}\right]$$

$$+ \gamma_2 f \left(\frac{\theta_i - \theta_{T2}}{\beta}\right) \cos \left[\omega_0 t + \phi(t) + \psi_{2i}\right] + n(t), \tag{A9}$$

where ψ_{1i} and ψ_{2i} are assumed to be uniformly distributed, independent random variables with

$$E \; (\psi_{1i} \; \psi_{1j}) = \frac{\pi^2}{3} \delta_{ij}. \tag{A10}$$

Also

$$E, (\psi_{1i} \; \psi_{2j}) = 0, \text{ all } i \text{ and } j. \tag{A11}$$

*R. Price, "Some Non-central F-Distributions Expressed in Closed Form," Biometrika 51, Nos. 1 — 2, 107 (1964).

Again the noise is white Gaussian with

$$E[n(t)n(u)] = \frac{N_0}{2}\,\delta\,(t-u). \tag{A12}$$

The quadrature components x_{ci} and x_{si} are again seen to be conditionally normal, that is, given ψ_{1i} and ψ_{2i},

$$\chi_{ci} \sim N\,(\mu_{ci}, 1) \tag{A13a}$$

and

$$\chi_{si} \sim N\,(\mu_{si}, 1), \tag{A13b}$$

where

$$\mu_{ci} = \frac{\gamma_1}{\sigma} f\left(\frac{\theta_i - \theta_{T1}}{\beta}\right) \cos\,\psi_{1i} + \frac{\gamma_2}{\sigma} f\left(\frac{\theta_i - \theta_{T2}}{\beta}\right) \cos\,\psi_{2i} \tag{A14a}$$

and

$$\mu_{si} = \frac{\gamma_1}{\sigma} f\left(\frac{\theta_i - \theta_{T1}}{\beta}\right) \sin\,\psi_{1i} + \frac{\gamma_2}{\sigma} f\left(\frac{\theta_i - \theta_{T2}}{\beta}\right) \sin\,\psi_{2i}. \tag{A14b}$$

The output of the envelope detector y_i is the sum of squares of two independent, conditionally normal random variables with nonzero mean and unit variance, and thus y_i is conditionally noncentral-chi-square distributed with two degrees of freedom and noncentrality parameter λ_{2i}, where

$$\lambda_{2i} = \frac{\gamma_1^2}{\sigma^2} f^2\left(\frac{\theta_i - \theta_{T1}}{\beta}\right) + \frac{\gamma_2^2}{\sigma^2} f^2\left(\frac{\theta_i - \theta_{T2}}{\beta}\right)$$
$$+ \frac{2\gamma_1\,\gamma_2}{\sigma^2} f\left(\frac{\theta_i - \theta_{T1}}{\beta}\right) f\left(\frac{\theta_i - \theta_{T2}}{\beta}\right) \cos\,(\psi_{1i} - \psi_{2i}). \tag{A15}$$

To obtain the unconditional distribution of y_i under H_2, it is necessary to average over the phase-difference variable, that is

$$p(y_i \mid H_2) = \int p(y_i \mid \psi_{1i}, \psi_{2i}, H_2)\, p(\psi_{1i}, \psi_{2i})\, d\psi_{1i}\, d\psi_{2i}. \tag{A16}$$

In view of the difficulty in evaluating Eq. (A16), it was decided to approximate the noncentrality parameter λ_{2i} of Eq. (A15) by its ensemble average:

$$\lambda_{2i} \approx \frac{\gamma_1^2}{\sigma} f^2\left(\frac{\theta_i - \theta_{T1}}{\beta}\right) + \frac{\gamma_2^2}{\sigma^2} f^2\left(\frac{\theta_i - \theta_{T2}}{\beta}\right). \tag{A17}$$

The unconditional distribution of y_i under H_2 is then noncentral chi-square with two degrees of freedom and with the noncentrality parameter of Eq. (A17).